

Chapter 7

Nucleon Spin Physics: Expectations through 2015

The next five years of the spin program will focus on longitudinally polarized $p + p$ collisions at $\sqrt{s} = 500$ GeV in order to improve constraints on the flavor-separated sea quark helicity distributions as well as probe $\Delta g(x)$ down to lower momentum fractions. Transversely polarized data taken at $\sqrt{s} = 200$ GeV and possibly lower energies will also considerably improve upon several transverse spin measurements made previously.

7.1 Flavor separation of the sea quark helicity distributions via W boson measurements

As W bosons are produced through a pure $V - A$ interaction, a beam of polarized protons of negative helicity essentially provides a beam of left-handed up quarks. As a manifestation of the maximal parity violation of the W bosons, they precisely couple only to left-handed particles. Therefore, when the up quarks collide with a \bar{d} anti-quark from an unpolarized proton to produce a W^+ boson, a very large and negative single-spin asymmetry should be seen when the decay positrons are in the forward direction of the polarized proton. This makes W production in polarized $p + p$ an ideal process to study the spin-flavor structure of the proton.

In PHENIX this will be done via the detection of high p_T electrons/positrons in the central arms from the decay $W^\pm \rightarrow e^\pm \nu$ and of high p_T muons in the muon arms from $W^\pm \rightarrow \mu^\pm \nu$. Our simultaneous coverage in forward, backward, and central rapidity will provide a powerful means of determining the quantities $\Delta\bar{u}/\bar{u}$, and $\Delta\bar{d}/\bar{d}$ in the parton momentum range $0.05 < x_{Bj} < 0.6$. Almost direct quark/anti-quark separation is possible with forward/backward leptons from W- production in the PHENIX muon arms due to much larger quark density vs anti-quark density at large momentum transfer. In this case, $A_L(\text{forward } W^- \rightarrow \mu^-) \approx \Delta d/d$. Similarly, $A_L(\text{backward } W^- \rightarrow \mu^-) \approx \Delta\bar{u}/\bar{u}$. Additionally, measurement of W^+ production will give access to $\Delta u/u$ and $\Delta\bar{d}/\bar{d}$. However, due to the fixed neutrino helicity, the flavor contributions in forward and backward rapidity are mixed. Similarly, the parity-

7.1. FLAVOR SEPARATION OF THE SEA QUARK HELICITY DISTRIBUTIONS VIA W BOSON ME.

29 violating asymmetry of W^+ production in central rapidity combines contributions from both
 30 u and \bar{d} polarizations, and from d and \bar{u} polarizations in W^- production. In general, the
 31 asymmetry is the superposition of the two cases shown in Figure 7.1:

$$A_L^{W^+} = \frac{\Delta u(x_1)\bar{d}(x_2) - \Delta\bar{d}(x_1)u(x_2)}{u(x_1)\bar{d}(x_2) + \bar{d}(x_1)u(x_2)}, \quad (7.1)$$

32 with the asymmetry for W^- production given by exchanging u and d .

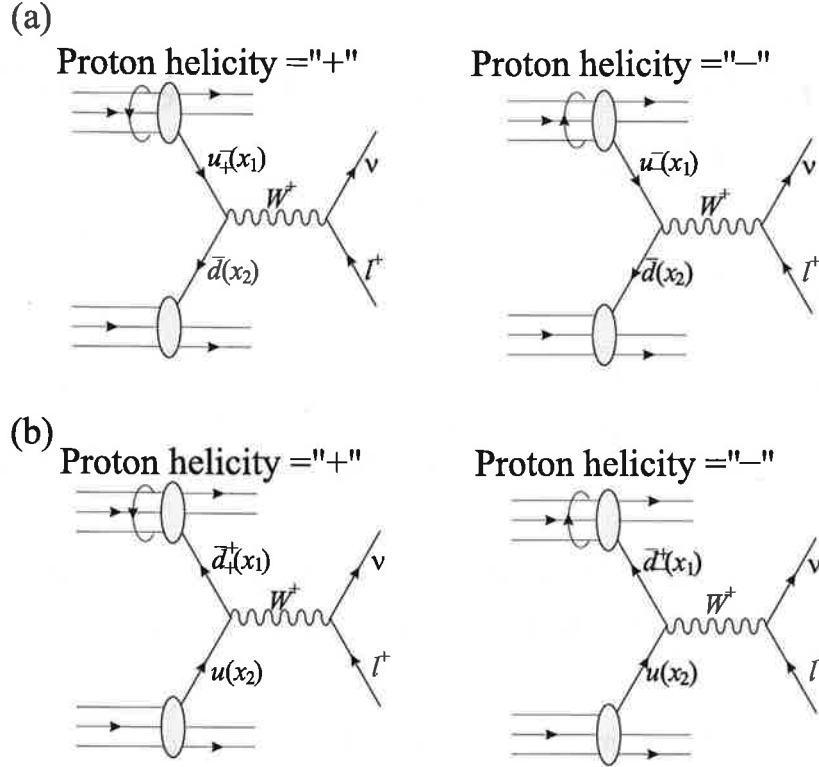


Figure 7.1: Leading-order production of a W^+ in a single-longitudinally polarized $p + p$ collision: (a) Δu is probed. (b) $\Delta\bar{d}$ is probed.

33 Present knowledge of flavor-separated quark helicity distributions comes from combined
 34 information from DIS measurements on polarized proton and neutron targets as well as
 35 polarized semi-inclusive DIS measurements, in which a variety of final-state hadron species
 36 are used to tag different quark flavors [120, 121]. Probing the flavor separation of the quark
 37 helicity distributions at RHIC via W boson production is complementary to these semi-
 38 inclusive DIS measurements in that the distributions are probed at a significantly higher
 39 energy scale (m_W^2), and no reliance on FFs is necessary.

40 RHIC had a first exploratory run at $\sqrt{s} = 500$ GeV in 2009, and PHENIX has already
 41 released results for both the $W^\pm \rightarrow e^\pm$ cross sections at this energy, shown in Figure 7.2, as
 42 well as A_L at midrapidity, with a clear parity-violating asymmetry observed, as can be seen
 43 in Figure 7.3. While in the 2009 run all experimental subsystems were in place to measure

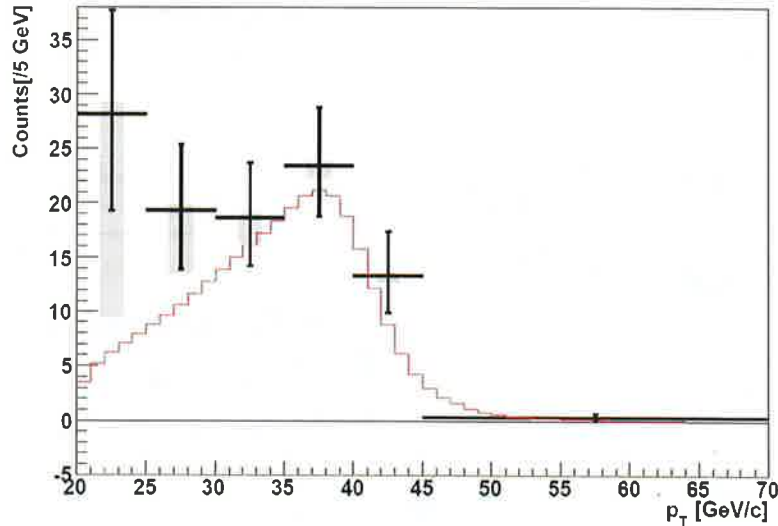


Figure 7.2: Midrapidity yield of candidate positrons from W^+ decay, measured in Run-09.

The gray bands reflect the range of background estimates used in the analysis.

Red histogram is NLO prediction [27] normalized for the integrated luminosity, corrected for the detector efficiency and acceptance, and smeared by the energy resolution of the calorimeter.

the W decay to electrons, an upgraded trigger is needed in order to measure $W^\pm \rightarrow \mu^\pm$,
described below.

at $\sqrt{s} = 200$ GeV operation

Muon trigger Measurements of parity violating spin asymmetries in W -production with the PHENIX muon arms require a first-level muon trigger that selects high momentum muons ($p > 10$ GeV/ c) and rejects the abundant muons from hadron decays, cosmic rays, and beam backgrounds. The existing muon trigger identifies muon candidates based on their ability to penetrate a sandwich of steel absorber and muon detector planes. Muons with momenta above $p > 2$ GeV/ c are selected. The resulting trigger rejection factor ranges from $200 < R < 500$, depending on the (varying) beam background levels. The muon trigger upgrade introduces tracking and timing information to a new set of muon trigger processors. The additional information will increase the muon trigger rejection by more than a factor 30.

see separate latex file

The PHENIX muon trigger upgrade has two components: (I) new front-end electronics for the muon tracking chambers to send tracking information to new dedicated muon trigger processors, and (II) two resistive plate chamber trigger detector stations in each muon arm: RPC-1 at the entrance and RPC-3 at the exit. The RPC stations provide both tracking and timing and are based on technology developed for the CMS muon trigger. The timing information adds background rejection power in the offline analysis, particularly to remove tracks due to cosmic rays, while making the online trigger much less sensitive to beam-related backgrounds.

The baseline muon trigger upgrade for Run-11 includes the new muon tracker trigger electronics for stations 1-3 and RPC-3 installed both in the south and north muon spec-

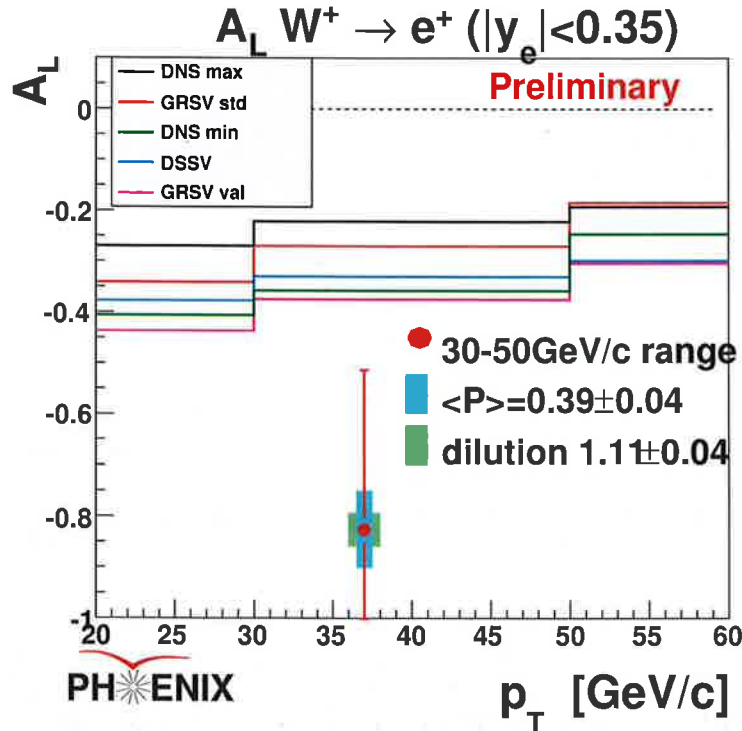


Figure 7.3: Parity-violating asymmetry of positrons from W^+ decay, measured in Run-09.

66 trometers. Also required are the first level trigger processors (LL1) that combine muon
 67 tracker hit and RPC hit information and perform the actual muon trigger algorithm.

68 The muon tracker trigger electronics for all stations have already been installed and tested
 69 successfully, including complete trigger chain tests with the muon tracker trigger electronics
 70 and the LL1 trigger processors. Figure 7.4 shows the RPC Station 3 detectors, which were
 71 successfully installed in the North muon arm during the shutdown prior to Run-10.

72 The RPC-3 north front end electronics was installed during Run-10 using accelerator
 73 access days and initial testing has been carried out. Installation of RPC-3 south will be
 74 completed before the beginning of Run-11. RPC-1 chamber construction and installation in
 75 both arms will be completed before the start of Run-12.

76 Full suppression of offline backgrounds in the W-physics analysis also requires two new 35
 77 cm thick steel absorbers upstream of the PHENIX muon spectrometer arms. 1-2% of hadrons
 78 with low momentum punch through the central magnet yoke upstream of the PHENIX muon
 79 spectrometers. A small fraction of these hadrons decays into muons in the spectrometer
 80 magnet volume such that the upstream hadron track and the downstream decay muon track
 81 overall mimic a high momentum track. We have carried out detailed Monte Carlo simulations
 82 that identify false high p_T tracks as the dominant source of the off-line background. We have
 83 shown in simulations and through data taken with a prototype absorber in Run-09 that an
 84 absorber of two nuclear interaction lengths thickness reduces the background to acceptable



Figure 7.4: Installed RPC Detector for North muon trigger.

~~RHIC
polarization
development~~

85 levels. The new absorbers will be in place for Run-11.

86 **Projections for the next five years** We expect the next 500 GeV polarized $p + p$ run
87 to be in Run-11, and have set a goal of recording 50 pb^{-1} , followed by 100 pb^{-1} in Run-12.
88 It is imperative to collect sufficient data before 2013 to achieve NSAC milestone HP8, which
89 requires measurement of flavor-identified q and \bar{q} contributions to the spin of the proton via
90 the longitudinal-spin asymmetry of W production in calendar year 2013. We anticipate that
91 this milestone can probably be at least partially satisfied with with the requested luminosity;
92 the ultimate result will require 300 pb^{-1} integrated luminosity. In Runs 11-14, the beam
93 polarizations should be at least 50%, and increase to 60% as soon as possible.

94 Combining Run-11 and Run-12 500 GeV $p + p$ runs will provide 150 pb^{-1} integrated
95 luminosity. Should the background rejection prove difficult to achieve with offline cuts and
96 the absorber, the forward silicon vertex detector (fVTX) can be used for further rejection
97 power beginning in Run-12. In this case, a tighter vertex cut will be required, resulting in
98 approximately 50 pb^{-1} sampled in Run-12. More likely, we will be able to use events from
99 the entire collision vertex, resulting in the error bars shown in Figure 7.5 from the combined
100 Run-11 and Run-12 data sets. A signal-to-background ratio of 3.0 has been assumed, which
101 we hope to be able to achieve. The curves show the results of various pQCD fits including
102 different inclusive and semi-inclusive DIS data along with RHIC polarized $p + p$ data from
103 previous runs. It is clear that the 500 GeV data from PHENIX will have a substantial
104 impact.

105 The plots in Figure 7.6 show the current uncertainties obtained by a pQCD fit[120, 121]
106 to the world data from inclusive and semi-inclusive deep inelastic scattering. Figure 7.6

RHIC
1 Milestone?

due to
the limited
acceptance
coverage by
fVTX

Unless you describe the reason why we can achieve $S/N \approx 3$ w/o fVTX,
"More likely," is not scientific expression. More likely, we... \Rightarrow If we

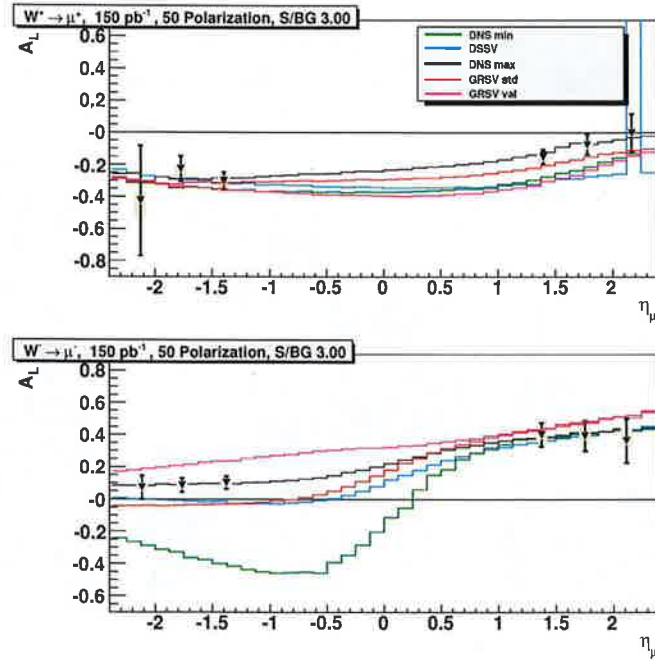


Figure 7.5: Expectation for uncertainties in W asymmetry measurements with 150 pb⁻¹ recorded with 50% polarization and S/B=3.0.

107 shows the impact of the W[±]A_L for 300 pb⁻¹ with a mean polarization of 60%. The W
 108 data reduce the uncertainties on the sea-quark polarizations for 0.05 < x < 0.6 significantly,
 109 furthermore serving as a set of complementary measurements to the ones in semi-inclusive
 110 DIS, as discussed above.

111 7.2 Improving constraints on $\Delta g(x)$

112 In recent years the golden channel at PHENIX to constrain the gluon polarization has been
 113 inclusive π^0 production. Through Run-9, PHENIX has recorded a total of approximately
 114 25-30 pb⁻¹ (summed over Runs 5, 6, and 9) of polarized p + p collisions at 200 GeV. Figure
 115 7.7 shows the current status of A_{LL} for this process.

116 Our goal at 200 GeV had been to record approximately 70 pb⁻¹, however it is clear that
 117 with currently achievable luminosity meeting this goal would require several more years. The
 118 measured double spin asymmetry in inclusive π^0 production, A_{LL}^{π⁰}, is consistent with zero in
 119 the transverse momentum range 1 < p_T < 10 GeV/c, limiting the gluon spin contribution to
 120 the proton spin in the parton momentum range 0.02 < x_g < 0.3 to -0.7 < ΔG^[0.02,0.3] < 0.5
 121 at 3σ[23]. Even though the measurements have become very precise, and have started to
 122 constrain the gluon polarization [121] there remain several open questions, like what is the
 123 gluon polarization at low-x, where the gluon density in the proton is biggest and can higher
 124 twist contributions become important as the leading twist contribution is small? PHENIX

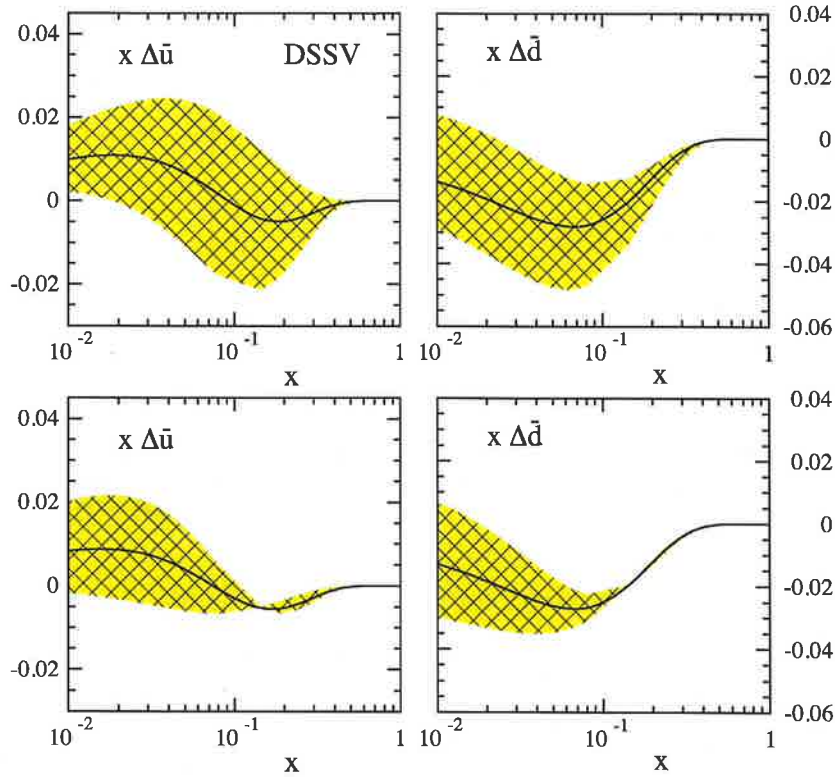


Figure 7.6: Upper plot: Uncertainty band on $x\Delta\bar{u}$ and $x\Delta\bar{d}$ resulting from the current fit to the world data from inclusive and semi-inclusive DIS by DSSV[120, 121]. Lower plot: Improvement in the uncertainties adding constraint from $W^\pm A_L$ measured with 300 pb^{-1} of 500 GeV $p + p$ collisions with 60% polarization.

125 plans to move forward with the accumulation of statistics at 500 GeV over the next several
 126 years to extend the study of gluon polarization to smaller x_g while beginning exploration of
 127 the spin polarization of \bar{u} , and \bar{d} quarks via the parity-violating asymmetry in and W boson
 128 production.

129 Figure 7.8 shows that the two lowest x points reached via midrapidity π^0 production at
 130 500 GeV fall below the lowest x points in the 200 GeV data, extending our sensitivity down
 131 to $x < 0.02$. The expected magnitude of the asymmetries at \sqrt{s} 200 GeV and 500 GeV
 132 can be related to good approximation by using x_T -scaling ($x_T = 2p_T/\sqrt{s}$).

133 Figure 7.9 shows the expected uncertainties in $A_{LL}^{\pi^0}$ as a function of p_T at 500 GeV
 134 assuming we reach 350 pb^{-1} (130 pb^{-1}) recorded in the years 2011 - 2015 within the standard
 135 $\pm 30 \text{ cm}$ ($\pm 10 \text{ cm}$) vertex and a polarization of 50%. The vertex distribution in the central
 136 detector is limited to $\pm 10 \text{ cm}$ compared to the regular $\pm 30 \text{ cm}$, because with the installation
 137 of the new vertex detector in summer 2010, there will be considerable material thickness
 138 due to the vertex detector support structure beyond the $\pm 10 \text{ cm}$ vertex region. As this is
 139 a double spin asymmetry, it is important to have the highest polarization achievable; the
 140 difference between 50% (40%) and 60% polarization is the equivalent to recording more than

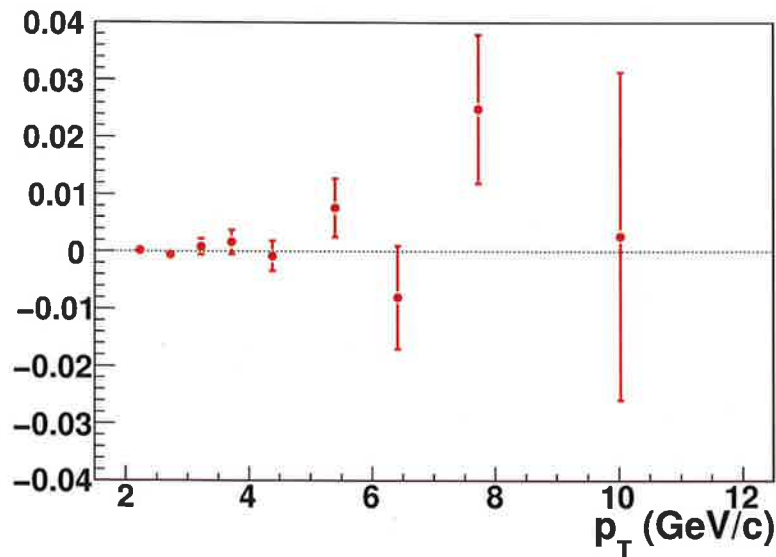


Figure 7.7: The double spin asymmetry for inclusive π^0 production combined for the years 2005 - 2009.

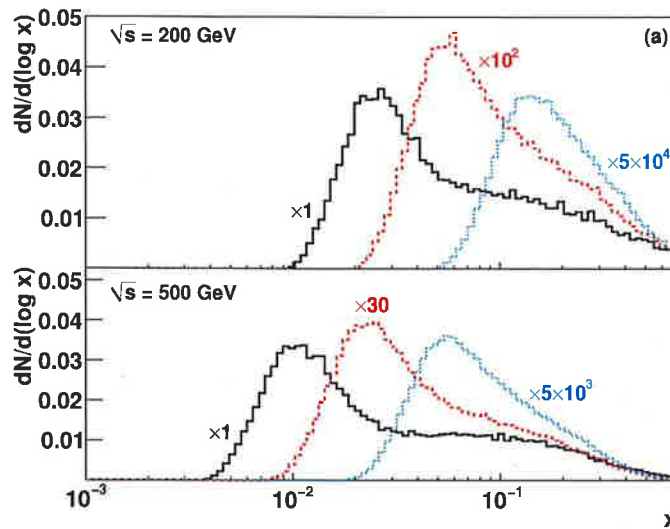


Figure 7.8: x range covered by π^0 at different p_T in 200 and 500 GeV collisions. Black, red, and blue curves correspond to 2-2.5, 4-5, and 9-12 GeV/c p_T , respectively. The different x -ranges are multiplied by some factor to make them better visible during comparison.

141 a factor of two (five) times higher luminosity. This is especially important ^{for the measurement} measuring at
 142 $\sqrt{s}=500$ GeV vs. 200 GeV as the unpolarized cross section in the denominator of $A_{LL}^{\pi^0}$ is
 143 growing much fast due to the strongly rising gluon and sea quark densities as the polarized
 144 cross section, so the expected asymmetries at low p_T are very small.

This sentence is getting too long.
 May be better to split it into two separate ones.

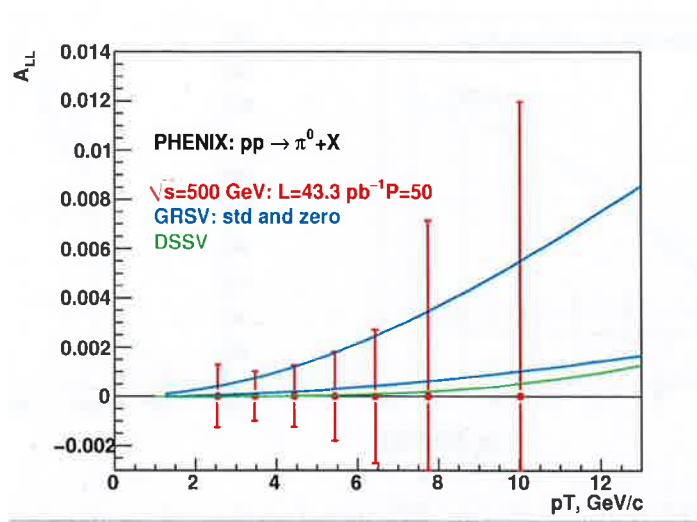


Figure 7.9: Expected uncertainties in $A_{LL}^{\pi^0}$ as a function of p_T for a recorded luminosity of 130 pb^{-1} and a polarization of 0.5. Only collisions with vertex inside $\pm 10 \text{ cm}$ are included.

145 Another possibility is to increase the x -range to lower x by going to forward rapidities
 146 ($x = Q/\sqrt{s} \cdot e^y$). In principle, a forward upgrade to the PHENIX experiment as discussed
 147 in Section ?? will allow us to greatly extend the x -range of PHENIX's measurements and
 148 provide information on the x dependence of ΔG . Despite the fact that the gluon polarization
 149 appears best constrained and falls off with decreasing x , the integral, ΔG , is dominated by
 150 contributions from $x < 0.1$ since this is the region where the gluons are most abundant. It
 151 is thus important to measure ΔG to values of x as far below 0.1 as feasible. Historically it is
 152 interesting to note that the quark spin crisis only arose from EMC [84] measurement of quark
 153 spin contributions and the extrapolation of PDF's to low x . Extrapolations of the SLAC [89]
 154 data alone led to results for the quark spin contribution consistent with expectations from
 155 naive quark models.

156 PHENIX has forward capabilities for ΔG already now by utilizing the Muon Piston
 157 Calorimeter (MPC) ($3.3 < \eta < 3.7$) for measurements of the inclusive $A_{LL}^{\pi^0}$. Figure 7.10
 158 shows the uncertainties expected for $A_{LL}^{\pi^0}$ requiring $p_t(\pi^0) > 3 \text{ GeV}$ and a sampled integrated
 159 luminosity of 100 pb^{-1} . Also shown are the expected uncertainties for a gluon polarization
 160 based on DSSV and GS-C. We are aware of the fact that GS-polarized parton distributions
 161 are completely outdated, but as the low- x behaviour for $\Delta g(x)$ is unknown, GS-C is an
 162 example for a polarized gluon pdf, which does have a slower behaviour for $\Delta g(x) \rightarrow 0$ as
 163 x goes to zero. But even for this extreme behaviour of GS-C the asymmetries are only on
 164 the 10^{-4} level. The measurement of such small asymmetries with good statistical precision
 165 requires excellent control of all the systematic uncertainties, i.e. relative luminosity on this
 166 level of the asymmetry, to have an efficient trigger and enough band-width in the DAQ to
 167 sample enough data in this kinematic region. In the right plot of Figure 7.10 it is shown how
 168 this measurement extends the current x -range indicated by the yellow band to $x \sim 10^{-3}$.

169 Extending the x -range is extremely important, but equally important is to study the

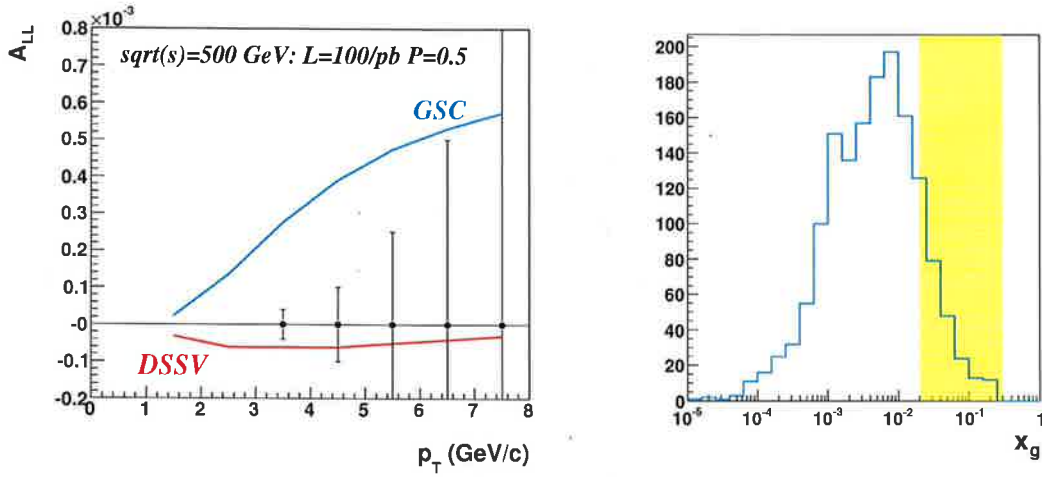


Figure 7.10: Expected uncertainties in A_{LL}^0 as a function of p_T measured with the MPC for an integrated sampled luminosity of 100 pb^{-1} . Also shown is the x -range covered by this measurement. The yellow band indicates the x -range covered by measurements in the central arm.

170 gluon polarization by measuring different final states. Despite the fact that the statistical
 171 uncertainties might be larger, this will allow us to determine systematic uncertainties due
 172 to restrictions in the current theoretical models. For example, currently all extractions of
 173 the gluon polarization are made in **leading twist**, but the leading-twist cross-section is so
 174 small, higher-twist contributions could **become** important. An example for such an effect is
 175 the sizable A_N , which is predicted to be small in pQCD at leading-twist level. As it is very
 176 difficult to calculate such higher-twist contributions, the comparison of different final states
 177 allows one to test this experimentally as higher-twist contributions are process dependent.
 178 The higher luminosity of collisions at 500 GeV compared to 200 GeV will finally provide the
 179 possibility to measure some of these luminosity-challenged processes. The measurement of
 180 the direct photon asymmetry is put within reach, opening an independent determination of
 181 ΔG . At RHIC, direct photon production is dominated by quark-gluon Compton scattering
 182 ($qg \rightarrow q\gamma$) (see Figure 7.11), which ensures that the double spin asymmetries from direct
 183 photon production provide clean theoretical access to the gluon polarization $\Delta g/g$. An
 184 advantage is also that the double helicity asymmetry will be linear with gluon polarization;
 185 consequently, PHENIX will be able to constrain both the sign and value of ΔG through this
 186 channel.

187 Like for all other hard subprocesses helicity conservation at the quark-gluon vertex gives
 188 rise to a double spin asymmetry

$$A_{LL} \sim \frac{\Delta q_f(x_A)}{q_f(x_A)} \otimes \frac{\Delta g(x_B)}{g(x_B)} \otimes a_{LL}^{qg \rightarrow q\gamma}$$

189 from which $\Delta g/g$ can be extracted. The hard scattering asymmetry, denoted by $a_{LL}^{qg \rightarrow q\gamma}$,
 190 is calculated for the underlying quark-gluon Compton diagram with perturbative QCD.

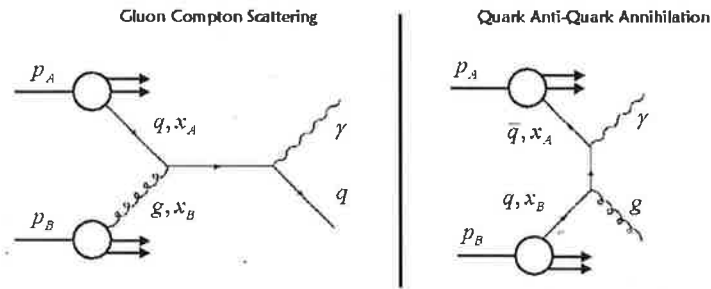


Figure 7.11: Direct photon production in the gluon Compton and quark anti-quark annihilation processes. The ratio of the two processes has been studied using PYTHIA and was found to be about 9:1.

191 Background from the quark anti-quark annihilation process has been studied using the event
 192 generator PYTHIA and was found to be small.

193 The measurement of a double spin asymmetry for the case of detecting only the direct
 194 photon, typically as a function of p_T , necessarily involves a convolution over the momentum
 195 fractions of the colliding partons; one compares the measurements to QCD predictions based
 196 on different models of the gluon distribution. Figure 7.12 shows the statistical uncertainties
 197 expected in 2015 for A_{LL}^γ . The plot clearly shows that a wider acceptance together with
 a higher integrated luminosity. In principle, if one could also detect the opposing quark

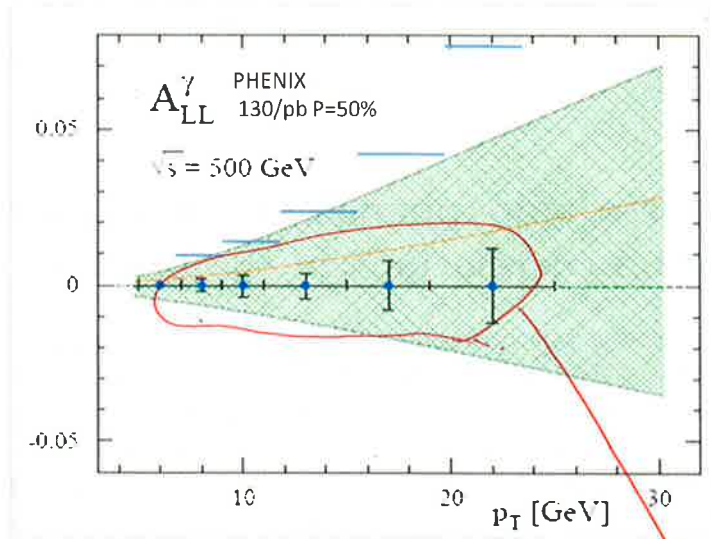


Figure 7.12: Expected uncertainties in A_{LL}^γ as a function of p_T for a recorded luminosity of 130 pb and a polarization of 0.5. Only collisions with vertex inside ± 10 cm are included. The blue horizontal bars indicate the expected statistical uncertainties vs. p_T . The orange curve corresponds to GRSV-std and the green band are the uncertainties corresponding to GRSV-max and GRSV-min.

then what are these error bars?

199 jet, then one may extract the the shape of the gluon distribution more directly, as the
 200 initial momentum fractions x_A and x_B are now known in LO (though the flavors and gluon
 201 combinations remain unknown and are summed over). This essentially allows a much more
 202 direct determination of the shape of the polarized gluon distribution. Unfortunately, the
 203 limited acceptance, $\eta \leq |0.35|$, of the current PHENIX detector and the absence of hadronic
 204 calorimetry presently make it challenging for us to reconstruct jets. The availability of the
 205 VTX detector after 2010 might allow to reconstruct a jet axis (via charged particles alone)
 206 in a wider acceptance $\eta \leq |1.0|$, but detailed studies are still underway. ~~With the PHENIX
 207 central detector upgrade the direct photon channel becomes much easier accessible ??.~~

208 With the installation of the vertex and forward vertex silicon detectors in PHENIX an-
 209 other channel sensitive to the gluon polarization becomes accessible. Open charm production
 210 at high energies as at RHIC is dominantly produced by gluon-gluon fusion. Measuring the
 211 double spin asymmetry for inclusive single electrons in the central arm and muons in the
 212 muon arms, or for the correlation between an electron in the central arm and a muon in the
 213 muon arms as well as two muons in the muon arms, allows one to produce another constraint
 214 on the gluon polarization. As the open charm mesons are produced in gluon-gluon fusion no
 215 access to the sign of the gluon polarization is possible. The vertex detectors are critical for
 216 this measurement, as only the requirement of a displaced vertex for the electron and muons
 217 can ensure that they are decay products from charmed mesons. Figure 7.13 shows the ex-
 218 pected magnitude [185] of $A_{LL}^{c\bar{c}}$ for single leptons and for correlations between leptons coming
 219 from charmed mesons based on the current knowledge of the gluon polarization from the
 220 fits to the world data. For all configurations the asymmetries based on the polarized gluon
 221 distribution from DSSV [120], which is constrained by the PHENIX $A_{LL}^{\pi^0}$ and the STAR A_{LL}^{jet}
 222 data, are on the 0.001 level. Therefore a measurement of $A_{LL}^{c\bar{c}}$, which gives a constraint for
 223 Δg in global pQCD fits like DSSV, needs either very high sampled luminosity or polarization
 224 or is not really feasible.

225 7.3 Transverse spin phenomena and partonic spin- 226 momentum correlations in the proton

227 In addition to the dedicated $p + p$ running at 500 GeV for the nucleon spin program, a
 228 significant amount of $p + p$ data at 200 GeV (40 pb^{-1} within $\pm 30 \text{ cm}$ in the years till 2015)
 229 and lower center-of-mass energies is anticipated over the next several years, driven primarily
 230 by the heavy ion program's requirements for $p + p$ reference data. This provides a good
 231 overlap with the luminosity needs for the transverse physics program at PHENIX. Currently
 232 the total recorded luminosity with transverse polarization was 8 pb^{-1} at 200 GeV with a
 233 beam polarization of 0.57 (2006) and 0.45 (2008). If a significantly higher statistics transverse
 234 data set with PHENIX were collected it would give the opportunity to pursue currently
 235 statistically challenged measurements (see Figure 7.14), with good statistical significance.
 236 For both the $A_N^{\pi^0}$ in the central arm and the MPC cluster single spin asymmetry it would be
 237 extremely interesting to see the behaviour at higher p_T more clearly as theoretical models
 238 based on collinear pQCD predict a drop of A_N at high p_T . There are indications in the data,